

Other applications of the pinch technique

11.1 Introduction

The pinch technique (PT) makes it possible to understand many questions in a variety of gauge theories gauge invariantly, as we have already seen for QCD in Chapters 7, 8, and 9 and for the electroweak sector of the standard model (SM) theory in Chapter 10. This chapter goes into more detail on some physical questions in electroweak theory and thermal NAGTs¹ that were difficult to interpret in the conventional framework of Feynman graphs and sometimes resulted in unfounded attempts to find physical properties in gauge-dependent calculations. Different authors used different gauges and got different results, sometimes not even agreeing on the sign. The pinch technique has resolved these issues. We also mention some interesting results for NAGTs embedded in supersymmetric theories, where the pinch technique confirms a number of supersymmetry nonrenormalization relations among the contributions of scalars and fermions to the PT three-gluon vertex, already discussed in Chapter 2. At the level of off-shell Green's functions, these relations hold only for the pinch technique and not for the conventional gauge-dependent Green's functions.

In this chapter, we cover the following subjects: (1) non-Abelian effective charges, (2) physical renormalization schemes versus \overline{MS} , (3) non-Abelian off-shell form factors, (4) the neutrino charge radius, (5) making gauge-particle resonance widths gauge invariant, (6) finite-temperature NAGTs, and (7) hints of supersymmetry in the PT Green's functions.

11.2 Non-Abelian effective charges

The extension of the concept of the effective charge from QED to non-Abelian gauge theories is, as the reader has already appreciated in Chapter 6, of

¹ The three-dimensional NAGTs of Chapter 9 carry the nonperturbative infrared singularities of finite-temperature gauge theories in four dimensions.

fundamental interest. This concept is even more important in theories involving unstable particles – for example, in the SM electroweak sector or disparate energy scales (e.g., grand unified theories). In the former, the Dyson summation of (appropriately defined) self-energies is needed to regulate the kinematic singularities of the corresponding tree-level propagators in the vicinity of resonances. In the latter, instead, the extraction of accurate low-energy predictions requires an exact treatment of threshold effects due to heavy particles: the construction of an effective charge, valid for all momenta and not just the asymptotic regime governed by the β function, constitutes the natural way to account for such threshold effects. As we know from Chapter 6, because the pinch technique cures the problem of the gauge-fixing parameter dependence of the conventionally defined gauge-boson self-energies, it is an ideal tool for the definition of physical effective charges in NAGTs.

11.2.1 Electroweak effective charges

In the electroweak sector of the SM, the various PT self-energies organize themselves into appropriate renormalization group (RG)-invariant combinations, essentially for the same fundamental reasons as in QCD [1]. The effective weak mixing angle $\bar{s}_w^2(q^2)$ corresponds to the RG-invariant combination

$$\bar{s}_w^2(q^2) = (s_w^0)^2 \left[1 - \left(\frac{c_w^0}{s_w^0} \right) \frac{\widehat{\Pi}_{AZ}^0(q^2)}{q^2 + \widehat{\Pi}_{AA}^0(q^2)} \right] = s_w^2 \left[1 - \left(\frac{c_w}{s_w} \right) \frac{\widehat{\Pi}_{AZ}(q^2)}{q^2 + \widehat{\Pi}_{AA}(q^2)} \right]. \tag{11.1}$$

Using the fact that $\widehat{\Pi}_{AZ}(0) = 0$, we may write $\widehat{\Pi}_{AZ}(q^2) = q^2 \widehat{\Pi}_{AZ}(q^2)$; then, at the one-loop level, $\bar{s}_w^2(q^2)$ reduces to

$$\bar{s}_w^2(q^2) = s_w^2 \left[1 - \left(\frac{c_w}{s_w} \right) \widehat{\Pi}_{AZ}(q^2) \right]. \tag{11.2}$$

Evidently, $\bar{s}_w^2(q^2)$ constitutes a universal modification to the effective vertex of the charged fermion.

Similarly, one may demonstrate that the combinations

$$g_w^2 \widehat{\Delta}_{WW}(q^2); \quad \frac{g_w^2}{c_w^2} \widehat{\Delta}_{ZZ}(q^2); \quad \frac{g_w^2}{M_W^2} \widehat{\Delta}_H(q^2), \tag{11.3}$$

are RG-invariant. The analog of Eq. (6.53) may be defined for the first two combinations. Specifically, retaining only the real parts of the corresponding self-energies, and casting $\Re e \widehat{\Pi}(q^2)_{ii}$ in the form $\Re e \widehat{\Pi}_{ii}(q^2) = \Re e \widehat{\Pi}_{ii}(M_i^2) + (q^2 - M_i^2) \Re e \widehat{\Pi}_{ii}(M_i^2)$, and then pulling out a common factor $(q^2 - M_i^2)$, we

obtain

$$\alpha_{w,\text{eff}}(q^2) = \frac{\alpha_w}{1 + \Re e \widehat{\Pi}_{WW}(q^2)}; \quad \alpha_{z,\text{eff}}(q^2) = \frac{\alpha_z}{1 + \Re e \widehat{\Pi}_{ZZ}(q^2)}, \quad (11.4)$$

where, as with $\widehat{\Pi}_{AZ}$, we factor out a mass-shell factor

$$\widehat{\Pi}_{ii}(q^2) = \frac{\widehat{\Pi}_{ii}(q^2) - \widehat{\Pi}_{ii}(M_i^2)}{q^2 - M_i^2}, \quad i = W, Z, \quad (11.5)$$

and $\alpha_w = g_w^2/4\pi$ and $\alpha_z = \alpha_w/c_w^2$.

Interestingly enough, the third RG-invariant combination in Eq. (11.3) leads to the concept of the *Higgs boson effective charge* [1]: the SM Higgs boson H couples universally to matter with an effective charge inversely proportional to its VEV.

11.2.2 Relation to physical cross sections

We consider the QED effective charge introduced in Chapter 6. This quantity displays a nontrivial dependence on the fermion masses m_f , which allows its reconstruction from physical amplitudes by resorting to the optical theorem and analyticity (i.e., dispersion relations). Given a particular contribution to the photon spectral function $\Im m \Pi(s)$, the corresponding contribution to $\Pi(q^2)$ can be reconstructed via a *once-subtracted dispersion relation* (see, e.g., de Rafael [2]). For example, for the one-loop contribution of the fermion f , choosing the on-shell renormalization scheme,

$$\Pi_{f\bar{f}}(q^2) = \frac{1}{\pi} q^2 \int_{4m_f^2}^{\infty} ds \frac{\Im m \Pi_{f\bar{f}}(s)}{s(s - q^2)}. \quad (11.6)$$

For $f \neq e$, $\Im m \Pi_{f\bar{f}}(s)$ is measured directly in the tree-level cross section for $e^+e^- \rightarrow f^+f^-$. For $f = e$, it is necessary to isolate the self-energy-like component of the tree-level Bhabha cross section. This is indeed possible because the self-energy-, vertex-, and boxlike components of the Bhabha differential cross section are *linearly independent functions* of $\cos \theta$; they may therefore be projected out by convoluting the differential cross section with appropriately chosen polynomials in $\cos \theta$. Thus, in QED, knowledge of the spectral function $\Im m \Pi_{f\bar{f}}(s)$, determined from the tree-level $e^+e^- \rightarrow f^+f^-$ cross sections, together with a measurement of the fine structure constant α , enables the construction of the one-loop effective charge $\alpha_{\text{eff}}(q^2)$ for all q^2 .

Keeping the QED example in mind, let us now turn to the case of the PT electroweak effective charges and study the procedure that would allow, at least in principle, the extraction of $\alpha_{z,\text{eff}}(q^2)$ from experiment [3]. In general, the renormalization of

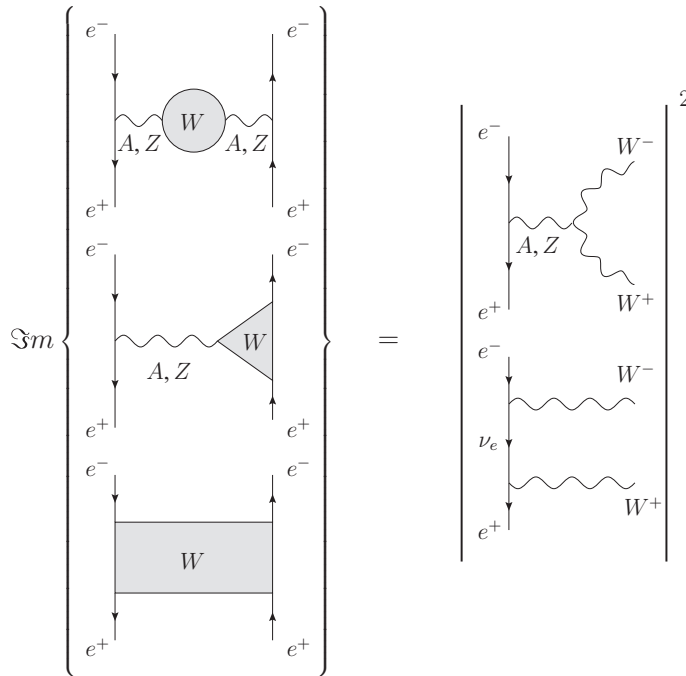


Figure 11.1. The relation between the imaginary parts of the subset of the W -related one-loop corrections to $e^+e^- \rightarrow e^+e^-$ and the tree-level process $e^+e^- \rightarrow W^+W^-$.

$\widehat{\Pi}_{ZZ}$ requires two subtractions: for mass and field renormalization. If we denote the subtraction point by s_0 , then the twice-subtracted dispersion relation corresponding to the renormalized W^+W^- contributions reads

$$\widehat{\Pi}_{ZZ}^{(WW)}(q^2) = \frac{1}{\pi}(q^2 - s_0)^2 \int_{4M_W^2}^{\infty} ds \frac{\Im m \widehat{\Pi}_{ZZ}^{(WW)}(s)}{(s - q^2)(s - s_0)^2}. \tag{11.7}$$

The property instrumental for the observability of $\alpha_{z,\text{eff}}(q^2)$ is that, in contrast to the conventional gauge-dependent self-energies, the absorptive parts of the PT self-energies appearing on the right-hand side (rhs) of Eq. (11.7) are directly related to components of the physical cross section $e^+e^- \rightarrow W^+W^-$ that are experimentally observable (see Figure 11.1). Indeed, as we have already seen in Chapter 10, the characteristic s - t cancellation, triggered by the longitudinal momenta of the on-shell polarization tensors, rearranges the tree-level cross section $e^+e^- \rightarrow W^+W^-$ into subamplitudes, which, through the use of the optical theorem, can be connected unambiguously with the absorptive parts of the one-loop PT Green's functions.

To simplify the algebra without compromising the principle, let us consider the limit of $e^+e^- \rightarrow W^+W^-$ when the electroweak mixing angle vanishes: $s_w^2 = 0$. In this limit, all photon-related contributions are switched off, and the two massive gauge bosons become degenerate ($M_Z = M_W \equiv M$). Let us denote by θ the center-of-mass scattering angle and set $x = \cos \theta$, $\beta = \sqrt{1 - 4M^2/s}$, and $z = (1 + \beta^2)/2\beta$. Then it is relatively straightforward to show that the differential tree-level cross section for $e^+e^- \rightarrow W^+W^-$ can be cast in the form [3]

$$(z - x)^2 \left(\frac{d\sigma}{dx} \right)_{s_w=0} = \frac{g^4}{64\pi} \frac{s\beta}{(s - M^2)^2} \theta (s - 4M^2) \sum_{i=1}^5 A_i(s) F_i(s, x), \quad (11.8)$$

where the $F_i(s, x)$, $i = 1, 2 \dots 5$, are linearly independent polynomials in x of maximum degree 4. The coefficients $A_1(s)$ and $A_2(s)$ contribute only to the self-energy-like component of the cross section, being related to $\Im m \widehat{\Pi}_{ZZ}^{(WW)}(s)$ by

$$\Im m \widehat{\Pi}_{ZZ}^{(WW)}(s)|_{s_w=0} = \frac{g^2}{4\pi} \beta s \left(A_1(s) + \frac{1}{3} A_2(s) \right). \quad (11.9)$$

To project the functions $A_i(s)$, we construct a further set of five polynomials $\widetilde{F}_i(s, x)$ satisfying the orthogonality conditions

$$\int_{-1}^1 dx F_i(s, x) \widetilde{F}_j(s, x) = \delta_{ij}. \quad (11.10)$$

The coefficient functions $A_i(s)$ may then be projected from the observable formed by taking the product of the differential cross section with the kinematic factor $(z - x)^2$:

$$\int_{-1}^1 dx \widetilde{F}_i(s, x) (z - x)^2 \left(\frac{d\sigma}{dx} \right)_{s_w=0} = \frac{g^4}{64\pi} \frac{s\beta}{(s - M^2)^2} A_i(s). \quad (11.11)$$

Thus it is possible to extract $\Im m \widehat{\Pi}_{ZZ}^{(WW)}(s)|_{s_w=0}$ directly from $d\sigma(e^+e^- \rightarrow W^+W^-)/dx|_{s_w=0}$.

Of course, to use the dispersion relation of Eq. (11.7) to compute $\widehat{\Pi}_{ZZ}^{(WW)}(q^2)$, one needs to integrate the spectral density $\Im m \widehat{\Pi}_{ZZ}^{(WW)}(s)$ over a large number of values of s . This in turn means that one needs experimental data for the process $e^+e^- \rightarrow W^+W^-$ for a variety of center-of-mass energies s , and for each value of s , one must repeat the procedure described earlier. Regardless of whatever practical difficulties this might entail, it does not constitute a problem of principle. Finally, the general case with $s_w^2 \neq 0$ requires, in addition, the observation of spin density matrices [4]; though technically more involved, the procedure is in principle the same.

11.3 Physical renormalization schemes versus $\overline{\text{MS}}$

It is no secret that the popular renormalization schemes, such as $\overline{\text{MS}}$ and $\overline{\text{DR}}$, convenient as they may be for formal manipulations, are plagued with persistent threshold and matching errors. The origin of these errors can be understood by noting that the aforementioned (unphysical) schemes implicitly integrate out all masses heavier than the physical energy scale until they are crossed, and then they turn them back on abruptly by means of a step function. Integrating out heavy fields, however, is only valid for energies well below their masses. This procedure is conceptually problematic because it does not correctly incorporate the finite probability that the uncertainty principle gives for a particle to be pair produced below threshold [5]. In addition, complicated matching conditions must be applied when crossing thresholds to maintain consistency for such desert scenarios. In principle, these schemes are only valid for theories in which all particles have zero or infinite mass or if one knows the full field content of the underlying physical theory.

Instead, in the physical renormalization scheme defined with the pinch technique, gauge couplings are defined directly in terms of physical observables, namely, the effective charges. The latter run smoothly over spacelike momenta and have non-analytic behavior only at the expected physical thresholds for timelike momenta; as a result, the thresholds associated with heavy particles are treated with their correct analytic dependence. In particular, particles will contribute to physical predictions even at energies below their threshold [5].

Historically, the gauge-invariant parametrization of physics offered by the pinch technique has been first systematized by Hagiwara et al. [6] and has led to an alternative framework for confronting the precision electroweak data with theoretical predictions. This approach resorts to the pinch technique to separate the one-loop corrections into gauge-fixing, parameter-independent universal (process independent) and process-specific pieces; the former are parametrized using the PT effective charges $\alpha_{\text{eff}}(q^2)$, $\bar{s}_w^2(q^2)$, $\alpha_{w,\text{eff}}(q^2)$, and $\alpha_{z,\text{eff}}(q^2)$, defined earlier. There is a total of nine electroweak parameters that must be determined in this approach: the eight universal parameters M_W , M_Z , $\alpha_{\text{eff}}(0)$, $\bar{s}_w^2(0)$, $\alpha_{w,\text{eff}}(0)$, $\alpha_{z,\text{eff}}(0)$, $\bar{s}_w^2(M_Z^2)$, and $\alpha_{z,\text{eff}}(M_Z^2)$ and one process-dependent parameter $\delta_b(M_Z^2)$, related to the form factor of the $Z\bar{b}_L b_L$ vertex.

Reference [6] explains in detail the advantage of their approach over the $\overline{\text{MS}}$ scheme. In particular, they emphasize that the nondecoupling nature of the $\overline{\text{MS}}$ forces one to adopt an effective field theory approach in which the heavy particles are integrated out of the action. The couplings of the effective theories are then related to each other by matching conditions ensuring that all effective theories give identical results at zero momentum transfer because the effects of heavy

particles in the effective light field theory must be proportional to q^2/M^2 , where M is the heavy mass scale. This procedure, however, is not only impractical in the presence of many quark and lepton mass scales but introduces errors because of the mistreatment of the threshold effects. In addition, direct use of the $\overline{\text{MS}}$ couplings leads to expressions in which the masses used for the light quarks are affected by sizable nonperturbative QCD effects.

The relevance of the effective charges in the quantitative study of threshold corrections due to heavy particles in grand unified theories (GUTs) was already recognized in [6], but it was not until a decade later that this was actually accomplished by Binger and Brodsky [5]. As was shown by these authors, the effective charges defined with the pinch technique furnish a conceptually superior and calculationally more accurate framework for studying the important issue of gauge-coupling unification. The main advantage of the effective charge formalism is that it provides a template for calculating all mass threshold effects for any given GUT; such threshold corrections may be instrumental in making the measured values of the gauge couplings consistent with unification.

In [5], the effective charges $\alpha_{\text{eff}}(q^2)$, $\alpha_{s,\text{eff}}(q^2)$, and the effective mixing angle $\bar{s}_w^2(q^2)$ were used to define new effective charges $\tilde{\alpha}_1(q^2)$, $\tilde{\alpha}_2(q^2)$, and $\tilde{\alpha}_3(q^2)$, which correspond to the standard combinations of gauge couplings used to study gauge-coupling unification. Specifically,

$$\tilde{\alpha}_1(q^2) = \left(\frac{5}{3}\right) \frac{\alpha_{\text{eff}}(q^2)}{1 - \bar{s}_w^2(q^2)}; \quad \tilde{\alpha}_2(q^2) = \frac{\alpha_{\text{eff}}(q^2)}{\bar{s}_w^2(q^2)}; \quad \tilde{\alpha}_3(q^2) = \alpha_{s,\text{eff}}(q^2). \quad (11.12)$$

The preceding couplings were used to obtain novel heavy and light threshold corrections, and the resulting impact on the unification predictions for a general GUT model was studied. Notice that even in the absence of new physics, i.e., using only the known SM spectrum, there are appreciable numerical discrepancies between the values of the conventional and PT couplings at M_Z (see Table I of [5]). Given that these values are used as initial conditions for the evolution of the couplings to the GUT scale, these differences alone may affect the unification properties of the couplings.

11.4 Gauge-independent off-shell form factors

It is well known that renormalizability and gauge invariance restrict severely the type of interaction vertices that can appear at the level of the fundamental Lagrangian. Thus, the tensorial possibilities allowed by Lorentz invariance are drastically reduced to relatively simple tree-level vertices. Beyond tree level, the

tensorial structures that have been so excluded appear due to quantum corrections; that is, they are generated from loops. This fact does not conflict with renormalizability and gauge invariance provided that the tensorial structures generated, not present at the level of the original Lagrangian, are UV finite; that is, no counterterms need be introduced to the fundamental Lagrangian proportional to the forbidden structures.

To fix the ideas, let us consider a concrete textbook example. In standard QED, the tree-level photon-electron vertex is simply proportional to γ_μ , whereas kinematically, one may have, in addition (for massive on-shell electrons, using the Gordon decomposition), a term proportional to $\sigma_{\mu\nu}q^\nu$ that would correspond to a nonrenormalizable interaction. Of course, the one-loop photon-electron vertex generates such a term: one has

$$\Gamma_\mu(q) = \gamma_\mu F_1(q^2) + \sigma_{\mu\nu}q^\nu F_2(q^2), \quad (11.13)$$

where the scalar cofactors multiplying the two tensorial structures are the corresponding form factors; they are in general nontrivial functions of the photon momentum transfer. $F_1(q^2)$ is the electric form factor, whereas $F_2(q^2)$ is the magnetic form factor. $F_1(q^2)$ is UV divergent and becomes finite after carrying out the standard vertex renormalization. On the other hand, $F_2(q^2)$ comes out UV finite, as it should, given that there is no term proportional to $\sigma_{\mu\nu}q^\nu$ (in configuration space) in the original Lagrangian, where a potential UV divergence could be absorbed. Of course, in the limit of $q^2 \rightarrow 0$, the magnetic form factor $F_2(q^2)$ reduces to the famous Schwinger anomaly [7].

At the level of an Abelian theory, such as QED, the preceding discussion exhausts more or less the theoretical complications associated with the calculation of off-shell form factors. However, in NAGTs, such as the electroweak sector of the SM, there is an additional important complication: the off-shell form factors obtained from the conventional one-loop vertex (and beyond) depend explicitly on the gauge-fixing parameter. This dependence disappears when going to the on-shell limit of the incoming gauge boson ($q^2 \rightarrow 0$ for a photon, $q^2 \rightarrow M_Z^2$ for a Z -boson, etc.) but is present for any other value of q^2 . This fact becomes phenomenologically relevant because one often wants to study the various form factors of particles that are produced in high-energy collisions, where the gauge boson mediating the interaction is far off shell. In the case of e^+e^- annihilation into heavy fermions, the value of q^2 must be above the heavy fermion threshold. For example, top quarks may be pair produced through the reaction $e^+e^- \rightarrow t\bar{t}$, with center-of-mass energy $s = q^2 \geq 4m_t^2$. In such a case, the intermediate photon and Z are far off-shell, and therefore the form factors F_i^V , appearing in the standard

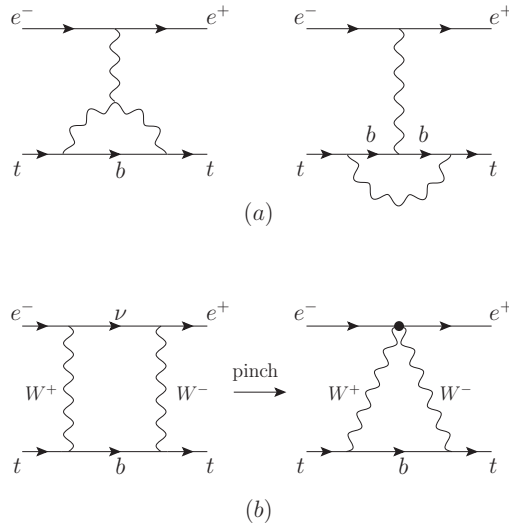


Figure 11.2. (a) The conventional one-loop vertex and (b) the vertexlike piece extracted from the box for $\xi \neq 1$.

decompositions

$$\Gamma_\mu^V(q^2) = \gamma_\mu F_1^V(q^2, \xi) + \sigma_{\mu\nu} q^\nu F_2^V(q^2, \xi) + \gamma_\mu \gamma_5 F_3^V(q^2, \xi) + \gamma_5 \sigma_{\mu\nu} q^\nu F_4^V(q^2, \xi), \tag{11.14}$$

depend explicitly on ξ , which stands collectively for ξ_W, ξ_Z, ξ_A , and $V = A, Z$.

The situation described is rather general and affects most form factors; very often, the residual gauge dependences have serious physical consequences. For example, the form factors display unphysical thresholds, have bad high-energy behavior, and sometimes are UV and IR divergent. The way out is to use the PT construction and extract the physical, gauge-independent form factors from the corresponding off-shell one-loop PT vertex (and beyond). Applying the pinch technique to the case of the form factors amounts to saying that one has to identify vertexlike contributions (with the appropriate tensorial structure corresponding to the form factor considered) contained in box diagrams, as shown in Figure 11.2. The latter, when added to the usual vertex graphs, render all form factors ξ independent and well behaved in all respects.

A particularly interesting case in which the pinch technique has been successfully applied is the study of the three-boson vertices AW^+W^- and ZW^+W^- , with the neutral gauge bosons off shell and the W pair on shell, or off shell and subsequently decaying to on-shell particles. Historically, the main motivation for exploring their properties was that they were going to be tested at LEP2 by direct W -pair production, proceeding through the process $e^+e^- \rightarrow W^+W^-$; their experimental scrutiny

could provide invaluable information on the non-Abelian nature of the electroweak sector of the SM. Particularly appealing in this quest has been the possibility of measuring anomalous gauge-boson couplings, that is, the appearance of contributions to AW^+W^- and ZW^+W^- not encoded in the fundamental Lagrangian of the SM. Linear combinations of these form factors are related to the magnetic dipole and the electric quadrupole moments of the W boson. Such contributions may originate from two sources: (1) from radiative corrections within the SM, (2) from physics beyond the SM, or both. Therefore, the first theoretical task is to carry out the necessary calculations for completing part (1).

Calculating the one-loop expressions for these anomalous form factors is a non-trivial task, both from technical and conceptual points of view. We focus for concreteness on the photon case. If one calculates just the Feynman diagrams contributing to the AW^+W^- vertex and then extracts from them the contributions to the relevant form factors, one arrives at expressions that are plagued with several pathologies, gauge-fixing parameter dependence being one of them. Indeed, even if the two W s are considered to be on-shell ($p_1^2 = p_2^2 = M_W^2$) because the incoming photon is not, there is no a priori reason why a gauge-fixing parameter-independent answer need emerge. Indeed, in the context of the renormalizable R_ξ gauges, the final answer depends on the choice of the gauge-fixing parameter ξ , which enters into the one-loop calculations through the gauge-boson propagators (W , Z , A , and unphysical would-be Goldstone bosons). In addition, as shown by an explicit calculation performed in the Feynman gauge ($\xi = 1$), the answer is infrared divergent and violates perturbative unitarity, that is, it grows monotonically for $q^2 \rightarrow \infty$ [8].

All the preceding pathologies may be cured if one uses the PT definition of the relevant (off-shell) gauge-boson vertices [9]. The application of the pinch technique identifies vertexlike contributions from the box graphs, as shown in Figure 11.3, which are subsequently distributed, in a unique way, among the various form factors. Thus one arrives finally at new expressions that are gauge-fixing parameter-independent, ultraviolet and infrared finite, and monotonically decreasing for large momentum transfers q^2 .

11.4.1 Neutrino charge radius

The neutrino electromagnetic form factor and the neutrino charge radius have constituted an important theoretical puzzle for more than three decades. Since well before the SM, it has been pointed out that radiative corrections will induce an effective one-loop $A^*(q^2)\nu\nu$ vertex, to be denoted by $\Gamma_{A\nu\bar{\nu}}^\mu$, with $A^*(q^2)$ an off-shell photon. Such a vertex would in turn give rise to a small but nonvanishing charge radius. Traditionally (and, of course, nonrelativistically and rather heuristically), this charge radius has been interpreted as a measure of the size of the neutrino

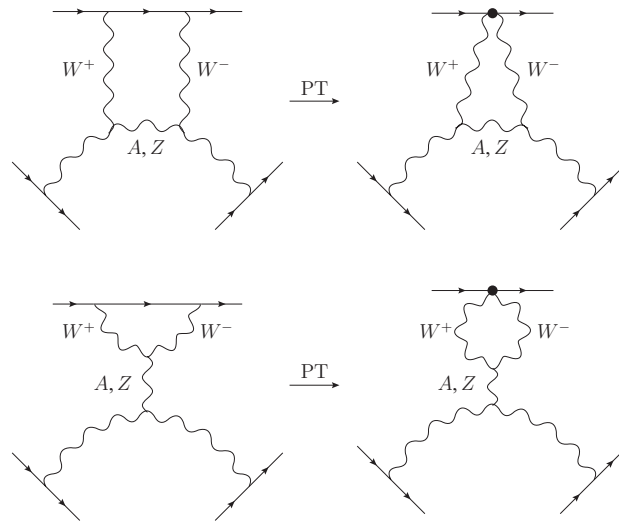


Figure 11.3. Two of the graphs contributing pinching parts to the gauge independent VW^+W^- vertex.

ν_i when probed electromagnetically, owing to its classical definition (in the static limit) as the second moment of the spatial neutrino charge density $\rho_\nu(\mathbf{r})$, i.e.,

$$\langle r_\nu^2 \rangle \sim \int d\mathbf{r} r^2 \rho_\nu(\mathbf{r}). \tag{11.15}$$

From the quantum field theory point of view, the neutrino charge radius is defined as follows. If we write $\Gamma_{A\nu\bar{\nu}}^\mu$ in the form

$$\Gamma_{A\nu\bar{\nu}}^\mu(q^2) = \gamma_\mu(1 - \gamma_5)F_D(q^2), \tag{11.16}$$

where $F_D(q^2)$ is the (dimensionless) Dirac electromagnetic form factor, then the neutrino charge radius is given by

$$\langle r_\nu^2 \rangle = 6 \left. \frac{\partial F_D(q^2)}{\partial q^2} \right|_{q^2=0}. \tag{11.17}$$

Gauge invariance (if not compromised) requires that in the limit $q^2 \rightarrow 0$, $F_D(q^2)$ must be proportional to q^2 ; that is, it can be cast in the form $F_D(q^2) = q^2 F(q^2)$, with the dimensionful form factor $F(q^2)$ being regular as $q^2 \rightarrow 0$. As a result, the q^2 contained in $F_D(q^2)$ cancels against the $(1/q^2)$ coming from the propagator of the off-shell photon, and one obtains effectively a contact interaction between the neutrino and the sources of the (background) photon, as would be expected from classical considerations.

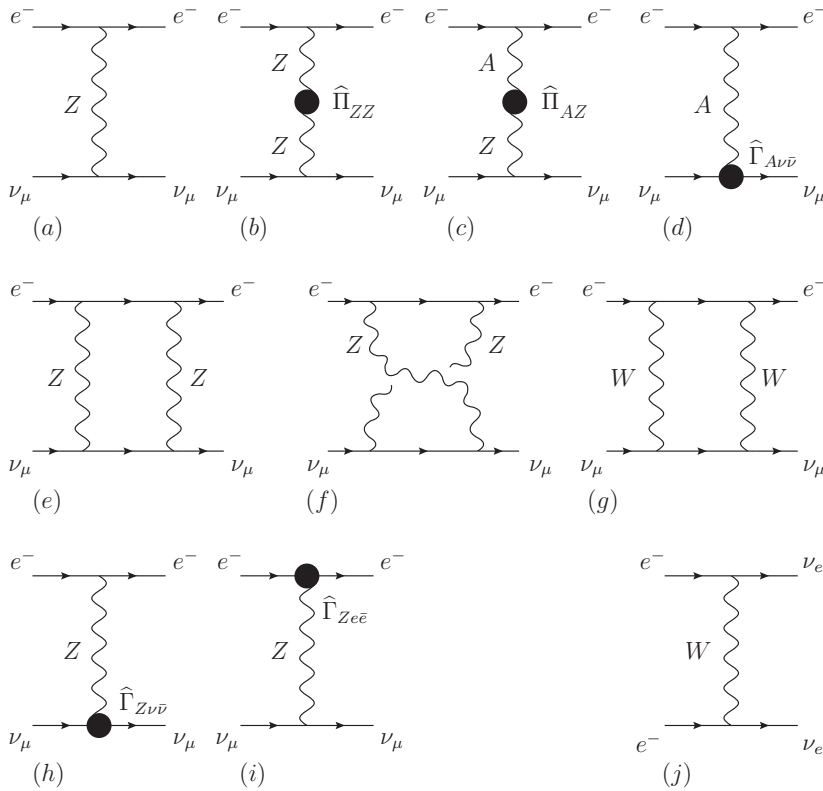


Figure 11.4. The electroweak diagrams contributing to the entire electron-neutrino scattering process at one loop. Diagram (j) (and the corresponding dressing) is absent when the neutrino species is muonic.

Even though, in the SM, the one-loop computation of the entire S -matrix element describing the electron-neutrino scattering, shown in Figure 11.4, is conceptually straightforward, the identification of a subamplitude that would serve as the effective $\Gamma_{A\nu\bar{\nu}}^\mu$ has been faced with serious complications, associated with the simultaneous reconciliation of crucial requirements such as gauge invariance, finiteness, and target independence. Various attempts to define the value of the neutrino charge radius within the SM from the one-loop $\Gamma_{A\nu\bar{\nu}}^\mu$ vertex calculated in the renormalizable (R_ξ) gauges reveal that the corresponding electromagnetic form factor depends explicitly on the gauge-fixing parameter ξ . In particular, even though in the static limit of zero momentum transfer, $q^2 \rightarrow 0$, the Dirac form factor vanishes and therefore is independent of ξ , its first derivative with respect to q^2 (which corresponds to the definition of the neutrino charge radius) continues to depend on it. Similar (and sometimes worse) problems occur in the context of other gauges (e.g., the unitary gauge). These complications have obscured the entire concept of a charge

radius for the neutrino and have cast serious doubt on whether it can be regarded as a genuine physical observable.

Of course, if a quantity is gauge dependent, it is not physical. But that the off-shell vertex is gauge dependent only means that it does not serve as a physical definition of the neutrino charge radius; it does not mean that an effective charge radius cannot be encountered that satisfies all necessary physical properties, gauge independence being one of them. Indeed, several authors have attempted to find a modified vertexlike amplitude that would lead to a consistent definition of the electromagnetic neutrino charge radius. The common underlying idea in all these works is to rearrange somehow the Feynman graphs contributing to the scattering amplitude of neutrinos with charged particles in an attempt to find a vertexlike combination that would satisfy all desirable properties. What makes this exercise so difficult is that in addition to gauge independence, a multitude of other crucial physical requirements need to be satisfied as well. For example, one should not enforce gauge independence at the expense of introducing target dependence. Therefore, a definite guiding principle is needed, allowing for the construction of physical subamplitudes with definite kinematic structure (i.e., self-energies, vertices, boxes).

The guiding principle in question has been provided by the pinch technique. As was shown in [10], the rearrangement of the physical amplitude $f^{\pm\nu} \rightarrow f^{\pm\nu}$, where f^{\pm} are the target fermions, into PT self-energies, vertices, and boxes conclusively settles the issue: the proper PT vertex with an off-shell photon and two on-shell neutrinos, denoted by $\widehat{\Gamma}_{A\nu_i\bar{\nu}_i}^{\mu}$, furnishes unambiguously and uniquely the physical neutrino charge radius.

Most recently, the issue of the neutrino charge radius was revisited in a series of papers [11, 12, 13]. There three important conceptual points have been conclusively settled:

1. As explained in [10], the box diagrams furnish gauge-dependent (propagator-like) contributions that are crucial for the gauge cancellations, but once these contributions have been identified and extracted, the remaining pure box cannot form part of the neutrino charge radius because it would introduce process dependence (in view of its nontrivial dependence on the target fermion masses, for one thing). The most convincing way to understand why the pure box could not possibly enter into the neutrino charge radius definition is to consider the case of right-handed polarized target fermions that do not couple to the W s: in that case, the box diagram is not even there. The gauge cancellations proceed differently because the coupling of the Z -boson to the target fermions is also modified [11, 12, 13].

2. The mixing self-energy $\widehat{\Pi}_{AZ}(q^2)$ should not be included in the definition of the neutrino charge radius either. The reason for this is more subtle: $\widehat{\Pi}_{AZ}(q^2)$ is not an RG-invariant quantity; adding it to the finite contribution coming from the proper vertex would convert the resulting neutrino charge radius into a μ -dependent, and therefore unphysical, quantity. Instead, $\widehat{\Pi}^{AZ}(q^2)$ must be combined with the appropriate Z -mediated tree-level contributions (which evidently do not enter into the definition of the charge radius) to form with them the RG-invariant combination $\bar{s}_w^2(q^2)$ of Eq. (11.2), whereas the ultraviolet-finite neutrino charge radius will be determined from the proper vertex only. Writing $\widehat{\Gamma}_{A\nu_i\bar{\nu}_i}^\mu = q^2 \widehat{F}_i(q^2) \gamma_\mu (1 - \gamma_5)$, the physical neutrino charge radius is then defined as $\langle r_{\nu_i}^2 \rangle = 6 \widehat{F}_i(0)$, and the explicit calculation yields

$$\langle r_{\nu_i}^2 \rangle = \frac{G_F}{4\sqrt{2}\pi^2} \left[3 - 2 \log \left(\frac{m_i^2}{M_W^2} \right) \right], \quad (11.18)$$

where $i = e, \mu, \tau$, m_i denotes the mass of the charged isodoublet partner of the neutrino under consideration and G_F is the Fermi constant.

3. The neutrino charge radius defined through the pinch technique may be extracted from experiment, at least in principle. One may express a set of experimental electron-neutrino cross sections in terms of the finite neutrino charge radius and the two additional gauge- and RG-invariant quantities, corresponding to the electroweak effective charge $\alpha_{z,\text{eff}}(q^2)$ and mixing angle $\bar{s}_w^2(q^2)$, defined earlier.

11.5 Resummation formalism for resonant transition amplitudes

The physics of unstable particles and the computation of resonant transition amplitudes have attracted significant attention in recent years because they are both phenomenologically relevant and theoretically challenging. The practical interest in the problem is related to the resonant production of various particles in all sorts of accelerators, most notably LEP1 and LEP2, the TEVATRON, and the LHC. From the theoretical point of view, the issue comes up every time fundamental resonances, i.e., unstable particles that appear as basic degrees of freedom in the original Lagrangian of the theory (as opposed to composite bound states), can be produced resonantly. The presence of such fundamental resonances makes it impossible to compute physical amplitudes for arbitrary values of the kinematic parameters, unless a resummation has taken place first. Simply stated, perturbation theory breaks down in the vicinity of resonances, and information about the dynamics to all orders needs to be encoded already at the level of Born amplitudes. The

difficulty arises that in the context of NAGTs, the standard Breit–Wigner resummation used for regulating physical amplitudes near resonances is at odds with gauge invariance, unitarity, and the equivalence theorem [14]. Consequently, the resulting Born-improved amplitudes in general fail to capture faithfully the underlying dynamics. It is therefore important to devise a self-consistent calculational scheme that manifestly preserves all relevant field-theoretic properties [1, 15, 16, 17, 18].

The mathematical expressions for computing transition amplitudes are ill defined in the vicinity of resonances because the tree-level propagator of the particle mediating the interaction (i.e., $\Delta = (s - M^2)^{-1}$) becomes singular as the center-of-mass energy approaches the mass of the resonance (i.e., as $\sqrt{s} \sim M$). The standard way to regulate this physical kinematic singularity is to use a Breit–Wigner type of propagator; this amounts essentially to the replacement (near the resonance) $(s - M^2)^{-1} \rightarrow (s - M^2 + iM\Gamma)^{-1}$, where Γ is the width of the unstable (resonating) particle. The presence of $iM\Gamma$ in the denominator prevents the amplitude from being divergent, even at physical resonance (i.e., when $s = M^2$).

The actual field-theoretic mechanism that justifies the appearance of the width is the Dyson resummation of the self-energy $\Pi(s)$ of the unstable particle, which amounts to the rigorous substitution $(s - M^2)^{-1} \rightarrow (s - M^2 + \Pi(s))^{-1}$. The running width of the particle is then defined as $M\Gamma(s) = \Im m \Pi(s)$, whereas the usual (on shell) width (see earlier) is simply its value at $s = M^2$.

It is relatively easy to realize that the Breit–Wigner procedure, as described earlier, is tantamount to a reorganization of the perturbative series. Resumming the self-energy $\Pi(s)$ amounts to removing a particular piece from each order of the perturbative expansion because from all the Feynman graphs contributing to a given order n , we only pick the part that contains the corresponding string of self-energy bubbles $\Pi(s)$ and then take $n \rightarrow \infty$. Notice, however, that the off-shell Green's functions contributing to a physical quantity, at any finite order of the conventional perturbative expansion, participate in a subtle cancellation that eliminates all unphysical terms. Therefore the act of resummation, which treats unequally the various Green's functions, is in general liable to distort these cancellations. To put it differently, if $\Pi(s)$ contains unphysical contributions (which would eventually cancel against other terms within a given order), resumming it naively would mean that these unphysical contributions would also undergo infinite summation (they now appear in the denominator of the propagator $\Delta(s)$). To remove them, one would have to add the remaining perturbative pieces to an infinite order, clearly an impossible task because the latter (boxes and vertices) do not constitute a resumable set. Thus, if the resummed $\Pi(s)$ contains such unphysical terms, one arrives at predictions plagued with unphysical artifacts. The crucial novelty introduced by the pinch technique is that the resummation of the (physical)

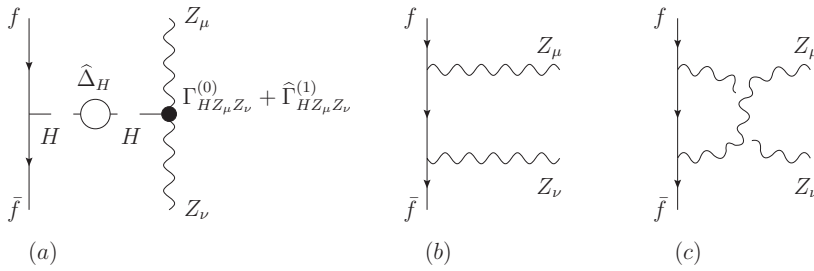


Figure 11.5. The amplitude for the process $f\bar{f} \rightarrow ZZ$. The s-channel graph (a) may become resonant and must be regulated by appropriate resummation of the Higgs propagator and dressing of the HZZ vertex.

self-energy graphs must take place only after the amplitude of interest has been cast via the PT algorithm into manifestly physical subamplitudes, with distinct kinematic properties, order by order in perturbation theory. Put in the language employed earlier, the PT ensures that all unphysical contributions contained inside $\Pi(s)$ have been identified and properly discarded before $\Pi(s)$ undergoes resummation.

11.5.1 An example

To get a flavor of the subtle interplay between the various physical constraints [1, 15, 16, 17, 18], we consider a concrete example. We study the process $f(p_1)\bar{f}(p_2) \rightarrow Z(k_1)Z(k_2)$, shown in Figure 11.5, and $s = (p_1 + p_2)^2 = (k_1 + k_2)^2$ is the center of mass energy squared. The tree-level amplitude of this process is the sum of an s- and t-channel contribution, denoted by \mathcal{T}_s and \mathcal{T}_t , respectively, given by

$$\begin{aligned} \mathcal{T}_s^{\mu\nu} &= \Gamma_{HZZ}^{\mu\nu} \Delta_H(s) \bar{v}(p_2) \Gamma_{Hf\bar{f}} u(p_1) \\ \mathcal{T}_t^{\mu\nu} &= \bar{v}(p_2) \left[\Gamma_{Zf\bar{f}}^\nu S^{(0)}(p_1 + k_1) \Gamma_{Zf\bar{f}}^\mu + \Gamma_{Zf\bar{f}}^\mu S^{(0)}(p_1 + k_2) \Gamma_{Zf\bar{f}}^\nu \right] u(p_1), \end{aligned} \tag{11.19}$$

where

$$\begin{aligned} \Gamma_{HZZ}^{\mu\nu} &= ig_w \frac{M_Z^2}{M_W} g^{\mu\nu}; & \Gamma_{Hf\bar{f}} &= -ig_w \frac{m_f}{2M_W} \\ \Gamma_{Zf\bar{f}}^\mu &= -i \frac{g_w}{c_w} \gamma_\mu (T_z^f P_L - Q_f s_w^2), \end{aligned} \tag{11.20}$$

are the tree-level HZZ , $Hf\bar{f}$, and $Zf\bar{f}$ couplings, respectively.

The s-channel contribution is mediated by the Higgs boson of mass M_H and becomes resonant if the kinematics are such that \sqrt{s} lies in the vicinity of M_H ;

in that case, the resonant amplitude must be properly regulated. The simplest way to accomplish this is to (1) Dyson-resum the one-loop PT self-energy of the (resonating) Higgs boson and (2) appropriately dress the tree-level vertex $\Gamma_{HZZ}^{\mu\nu}$, that is, by replacing in the amplitude the vertex $\Gamma_{HZZ}^{\mu\nu}$ with the one-loop PT vertex $\widehat{\Gamma}_{HZZ}^{\mu\nu}$.

We first see what happens if one attempts to regulate the resonant amplitude by means of the conventional one-loop Higgs self-energy in the R_ξ gauges. A straightforward calculation yields (tadpole and seagull terms omitted) [1, 18]

$$\begin{aligned} \Pi_{HH}^{(WW)}(s, \xi_W) &= \frac{\alpha_w}{4\pi} \left(\frac{s^2}{4M_W^2} - s + 3M_W^2 \right) B_0(s, M_W^2, M_W^2) \\ &+ \frac{\alpha_w}{4\pi} \left(\frac{M_H^4 - s^2}{4M_W^2} \right) B_0(s, \xi_W M_W^2, \xi_W M_W^2). \end{aligned} \quad (11.21)$$

We see that for $\xi_W \neq 1$, the term growing as s^2 survives and is proportional to the difference $B_0(s, M_W^2, M_W^2) - B_0(s, \xi_W M_W^2, \xi_W M_W^2)$. For any finite value of ξ_W , this term vanishes for sufficiently large s , that is, $s \gg M_W^2$ and $s \gg \xi_W M_W^2$. Therefore the quantity in Eq. (11.21) displays good high-energy behavior in compliance with high-energy unitarity. Notice, however, that the onset of this good behavior depends crucially on the choice of ξ_W . Because ξ_W is a free parameter and may be chosen to be arbitrarily large, but finite, the restoration of unitarity may be arbitrarily delayed as well. This fact poses no problem as long as one is restricted to the computation of physical amplitudes at a finite order in perturbation theory. However, if the preceding self-energy were to be resummed to regulate resonant transition amplitudes, it would lead to an artificial delay of unitarity restoration, which becomes numerically significant for large values of ξ_W . In addition, a serious pathology occurs for any value of $\xi_W \neq 1$, namely, the appearance of unphysical thresholds [15, 16, 17]. Such thresholds may be particularly misleading if ξ_W is chosen in the vicinity of unity, giving rise to distortions in the line shape of the unstable particle.

How does the situation change if, instead, we compute the corresponding part of the Higgs-boson self-energy in the BFM for an arbitrary value of ξ_Q ? Denoting it by $\widetilde{\Pi}_{HH}^{(WW)}(s, \xi_Q)$, and using the appropriate set of Feynman rules [19], we obtain

$$\widetilde{\Pi}_{HH}^{(WW)}(s, \xi_Q) = \Pi_{HH}(s, \xi_W \rightarrow \xi_Q) - \frac{\alpha_w}{4\pi} \xi_Q (s - M_H^2) B_0(s, \xi_Q M_W^2, \xi_Q M_W^2). \quad (11.22)$$

Evidently, away from $\xi_Q = 1$, $\widetilde{\Pi}_{HH}^{(WW)}(s, \xi_Q)$ displays the same unphysical characteristics mentioned earlier for $\Pi_{HH}^{(WW)}(s, \xi_W)$. Therefore, when it comes to the

study of resonant amplitudes, calculating in the BFM for general ξ_Q is as pathological as calculating in the conventional R_ξ gauges.

To solve these problems, one has simply to follow the PT procedure, within either gauge-fixing scheme R_ξ or background field method; identify the corresponding Higgs-boson-related pinch parts from the vertex and box diagrams; and add them to Eq. (11.21) or Eq. (11.22). Then a unique answer emerges, the PT one-loop Higgs boson self-energy, given by $\widehat{\Pi}_{HH}(q^2)$

$$\widehat{\Pi}_{HH}^{(WW)}(s) = \frac{\alpha_w}{16\pi} \frac{M_H^4}{M_W^2} \left[1 + 4 \frac{M_W^2}{M_H^2} - 4 \frac{M_W^2}{M_H^4} (2s - 3M_W^2) \right] B_0(s, M_W^2, M_W^2). \tag{11.23}$$

Setting $\xi_Q = 1$ in the expression of Eq. (11.22), we recover the full PT answer of Eq. (11.23), as expected. Clearly $\widehat{\Pi}_{HH}^{(WW)}(s)$ has none of the pathologies observed earlier.

We now turn to the way the PT-regulated amplitude satisfies the equivalence theorem [14]. This theorem states that at very high energies ($s \gg M_Z^2$), the amplitude for emission or absorption of a longitudinally polarized gauge boson becomes equal to the amplitude in which the gauge boson is replaced by the corresponding would-be Goldstone boson. The preceding statement is a consequence of the underlying local gauge invariance of the SM and holds to all orders in perturbation theory for multiple absorptions and emissions of massive vector bosons. Compliance with this theorem is a necessary requirement for any resummation algorithm because any Born-improved amplitude that fails to satisfy it is bound to be missing important physical information. The reason why most resummation methods are at odds with the equivalence theorem is that in the usual diagrammatic analysis, the underlying symmetry of the amplitudes is not manifest. Just as happens in the case of the optical theorem, the conventional subamplitudes, defined in terms of Feynman diagrams, do not satisfy the equivalence theorem individually. The resummation of such a subamplitude will in turn distort several subtle cancellations, thus giving rise to artifacts and unphysical effects. Instead, the PT subamplitudes satisfy the equivalence theorem individually; as usual, the only nontrivial step for establishing this is the proper exploitation of elementary Ward identities.

Turning to our explicit process $f(p_1)\bar{f}(p_2) \rightarrow Z(k_1)Z(k_2)$, the equivalence theorem states that the full amplitude $\mathcal{T} = \mathcal{T}_s + \mathcal{T}_t$ satisfies

$$\mathcal{T}(Z_L Z_L) = -\mathcal{T}(\chi\chi) - i\mathcal{T}(\chi z) - i\mathcal{T}(z\chi) + \mathcal{T}(\chi\chi), \tag{11.24}$$

where Z_L is the longitudinal component of the Z -boson, χ is its associated would-be Goldstone boson, and $z_\mu(k) = \varepsilon_\mu^L(k) - k_\mu/M_Z$ is the energetically suppressed

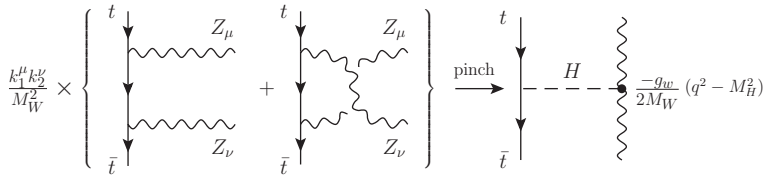


Figure 11.6. The Higgs-boson-related contribution extracted from the boxes through pinching; to get it, we must contract with both momenta.

part of the longitudinal polarization vector ε_μ^L . It is crucial to observe, however, that already at tree level, the conventional s - and t -channel subamplitudes \mathcal{T}_s and \mathcal{T}_t fail to satisfy the equivalence theorem individually [1, 18].

To verify this, one has to calculate $\mathcal{T}_s(Z_L Z_L)$, using explicit expressions for the longitudinal polarization vectors, and check if the answer obtained is equal to the Higgs-boson-mediated s -channel part of the left-hand side of Eq. (11.24). In particular, in the center-of-mass system, we have

$$z_\mu(k_1) = \varepsilon_\mu^L(k_1) - \frac{k_{1\mu}}{M_Z} = -2M_Z \frac{k_{2\mu}}{s} + \mathcal{O}\left(\frac{M_Z^4}{s^2}\right) \tag{11.25}$$

and an exactly analogous expression for $z_\mu(k_2)$. The residual vector $z_\mu(k)$ has the properties $k^\mu z_\mu = -M_Z$ and $z^2 = 0$. After a straightforward calculation, we obtain a new term $\mathcal{T}_s^P \sim (ig_w/2M_W)\bar{v}(p_2)\Gamma_{Hf\bar{f}}u(p_1)$ not found in Eq. (11.24)

$$\mathcal{T}_s(Z_L Z_L) = -\mathcal{T}_s(\chi\chi) - i\mathcal{T}_s(z\chi) - i\mathcal{T}_s(\chi z) + \mathcal{T}_s(zz) - \mathcal{T}_s^P, \tag{11.26}$$

where

$$\begin{aligned} \mathcal{T}_s(\chi\chi) &= \Gamma_{H\chi\chi} \Delta_H(s)\bar{v}(p_2)\Gamma_{Hf\bar{f}}^{(0)}u(p_1) \\ \mathcal{T}_s(z\chi) + \mathcal{T}_s(\chi z) &= [z_\mu(k_1)\Gamma_{HZ\chi}^\mu + z_\nu(k_2)\Gamma_{HZ\chi}^\nu]\Delta_H(s)\bar{v}(p_2)\Gamma_{Hf\bar{f}}u(p_1) \\ \mathcal{T}_s(zz) &= z_\mu(k_1)z_\nu(k_2)\mathcal{T}_s^{\mu\nu}(ZZ), \end{aligned} \tag{11.27}$$

with $\Gamma_{H\chi\chi} = -ig_w M_H^2/(2M_W)$ and $\Gamma_{HZ\chi}^\mu = -g_w(k_1 + 2k_2)_\mu/(2c_w)$. Evidently the presence of the term \mathcal{T}_s^P prevents $\mathcal{T}_s^H(Z_L Z_L)$ from satisfying the equivalence theorem. This is, of course, not surprising given that an important Higgs-boson-mediated s -channel part has been omitted. The momenta k_1^μ and k_2^ν , stemming from the leading parts of the longitudinal polarization vectors $\varepsilon_L^\mu(k_1)$ and $\varepsilon_L^\nu(k_2)$, extract such a term from $\mathcal{T}_t(Z_L Z_L)$ (see Figure 11.6); this term is precisely \mathcal{T}_s^P and must be added to $\mathcal{T}_s(Z_L Z_L)$ to form a well-behaved amplitude at high energies. In other words, the amplitude

$$\widehat{\mathcal{T}}_s(Z_L Z_L) = \mathcal{T}_s(Z_L Z_L) + \mathcal{T}_s^P \tag{11.28}$$

satisfies the equivalence theorem by itself (see Eq. (11.24)).

In fact, this crucial property persists after resummation – thanks to the Ward identities satisfied by the PT vertices. As shown in Figure 11.5(a), the resummed amplitude, to be denoted by $\overline{\mathcal{T}}_s(Z_L Z_L)$, is constructed from $\mathcal{T}_s(Z_L Z_L)$ in Eq. (11.19) by replacing $\Delta_H(s)$ with the resummed Higgs-boson propagator $\widehat{\Delta}_H(s)$ and $\Gamma_{HZZ}^{\mu\nu}$ with the expression $\Gamma_{HZZ}^{\mu\nu} + \widehat{\Gamma}_{HZZ}^{\mu\nu}$, where $\widehat{\Gamma}_{HZZ}^{\mu\nu}$ is the one-loop HZZ vertex calculated within the pinch technique. It is then straightforward to show that the Higgs-mediated amplitude $\widetilde{\mathcal{T}}_s(Z_L Z_L) = \overline{\mathcal{T}}_s(Z_L Z_L) + \mathcal{T}_s^P$ respects the equivalence theorem individually; to that end, we only need to employ PT Ward identities such as

$$\begin{aligned}
 k_{2\nu} \widehat{\Gamma}_{HZZ}^{\mu\nu}(q, k_1, k_2) + i M_Z \widehat{\Gamma}_{HZ\chi}^\mu(q, k_1, k_2) &= -\frac{g_w}{2c_w} \widehat{\Pi}_{Z\chi}^\mu(k_1) \\
 k_{1\mu} \widehat{\Gamma}_{HZ\chi}^\mu(q, k_1, k_2) + i M_Z \widehat{\Gamma}_{H\chi\chi}(q, k_1, k_2) &= -\frac{g_w}{2c_w} [\widehat{\Pi}_{HH}(q^2) + \widehat{\Pi}_{\chi\chi}(k_2^2)].
 \end{aligned}
 \tag{11.29}$$

In addition to the preceding issues, scattering amplitudes ought to be RG invariant; that is, they should not depend on the renormalization point μ chosen to carry out the subtractions nor on the renormalization scheme ($\overline{\text{MS}}$, on-shell scheme, momentum subtraction, etc.). This property must remain true in the vicinity of resonances, i.e., after resummation. To see how this happens for the process at hand, note that after the PT rearrangement, the resulting amplitude is decomposed into three individually RG-invariant parts:

1. A universal (process-independent) part, corresponding to the Higgs-boson effective charge, namely, the RG-invariant combination $(g_w^2/M_w^2)\widehat{\Delta}_H$, defined in Eq. (11.3); the line shape of the Higgs boson, being a universal quantity, must be obtained precisely from this part.
2. A process-dependent part, composed of the vertex corrections and the wave function renormalization of the external particles, which is RG invariant because of Abelian Ward identities.
3. A process-dependent part, coming from ultraviolet finite boxes; this is trivially RG invariant because it is ultraviolet finite and does not get renormalized.

Finally, on physical grounds, one expects that, far from the resonance, the Born-improved amplitude must behave exactly as its tree-level counterpart. In fact, a self-consistent resummation formalism should have this property built in; that is, far from resonance, one should recover the correct high-energy behavior without having to reexpand the Born-improved amplitude perturbatively. Recovering the correct asymptotic behavior is particularly tricky, however, when the final

particles are gauge bosons. The exact mechanism that enforces the correct high-energy behavior of the Born-improved amplitude, when the PT width and vertex are used, has been studied in detail in [20] for the specific process considered here.

11.6 The pinch technique at finite temperature

Finite-temperature gauge theories are a large and complicated subject (see, e.g., Gross et al. [21]) for which the pinch technique is useful. In Chapter 9 we mentioned the relationship of $d = 3$ gauge theories to $d = 4$ gauge theories at very high temperature, where a hierarchy of scales, based on the smallness of the coupling, made it possible to ignore chromoelectric fields and other phenomena. There are, in principle, three scales (besides momenta) in a thermal $SU(N)$ NAGT: the temperature T itself, $(Ng^2)^{1/2}T$, and Ng^2T . (We ignore factors such as $1/4\pi$ that may or may not occur in particular applications, although these can be very important.) By g we mean the four-dimensional coupling as a function of T (and other variables, if needed). The so-called magnetic mass of a thermal NAGT scales with Ng^2T ,² and the scale $(Ng^2)^{1/2}T$ appears as the scale of mass of the longitudinal electric degrees of freedom (the Debye or plasmon mass). In QCD, where the coupling decreases as T increases, or in EW theory, with its small coupling, these three scales should obey $T > (Ng^2)^{1/2}T > Ng^2T$, although this is not necessarily the case in any particular real-world application. Clearly the smallest scale, Ng^2T , sets the scale for infrared-dominated phenomena. Nonperturbative infrared phenomena at high T occur even for gauge theories normally thought of as weakly coupled such as the electroweak part of the standard model. Indeed, this theory is weakly coupled at low temperatures because of Higgs mass generation but strongly coupled at large T , where the Higgs VEV vanishes and the electroweak gauge bosons are perturbatively massless.

In the period 1980–1995, there were many attempts at calculating such quantities as the thermal β function and thermal plasmon³ damping rate with standard Feynman-graph techniques, nearly all of which were plagued with gauge dependence. In an attempt to resolve this and other problems, some people argued for using the Batalin–Vilkovisky approach – in the Landau gauge – and others argued for using the background field method – in an arbitrary covariant gauge (see Elmfors and Kobes [22] for such calculations and references to other authors). But because PT principles were not invoked, the methods used were dependent on gauge, just as

² Just as in $d = 4$, the mass runs and decreases at large momentum, as signaled by a magnetic condensate $\langle \text{Tr } G_{ij}^2 \rangle$. Recall that in Chapter 9 we proved that such a condensate exists in three dimensions.

³ The plasmon is essentially the longitudinal electric degree of freedom with its Debye mass.

were the usual Feynman-gauge approaches. One notable exception is the work of Braaten and Pisarski [23, 24, 25] on hard thermal loops, which we discuss briefly later on.

In Section 11.7, we briefly review the Matsubara decomposition of a thermal field theory into an infinite set of coupled $d = 3$ field theories labeled by an integer K for bosons or $K + 1/2$ for fermions. In each $d = 3$ theory, the corresponding fields have mass $2\pi T|K|$ (bosons) or $2\pi T|K + 1/2|$ (fermions). It follows that for all except the $K = 0$ bosonic sector, the basic scale of these field theories is T itself; all infrared nonperturbative phenomena come from the $K = 0$ sector of an NAGT. Moreover, as we will see, the coupling of any of these theories is $g^2 T$. In particular, the $K = 0$ sector is just the $d = 3$ NAGT of Chapter 9, with the replacement of the coupling g_3^2 by $g^2 T$, the lowest available scale. The characteristic dimensionless parameter of any of these field theories is $Ng^2 T/k$ at momentum scale k . Because the minimum momentum scale is a particle mass, it follows that the $K = 0$ sector is strongly coupled (dimensionless parameter of $\mathcal{O}(1)$), but this parameter is $\mathcal{O}(Ng^2)$ for all other sectors, possibly allowing for a perturbative expansion.⁴

11.7 Basic principles of thermal field theory

Consider the partition function of a bosonic quantum theory:

$$\mathcal{Z} = \text{Tr} e^{-\beta H} = \int [d\phi(\vec{x})] \langle \phi(\vec{x}) | e^{-\beta H} | \phi(\vec{x}) \rangle, \quad (11.30)$$

where $\beta = 1/T$, and write this as a path integral for a generic field theory over field coordinates at zero time. The matrix element has a standard path integral representation:

$$\langle \phi(\vec{x}) | e^{-\beta H} | \phi(\vec{x}) \rangle = \int [d\Phi] \exp \left[- \int \mathcal{L}_E \right], \quad (11.31)$$

where \mathcal{L}_E is the Euclidean Lagrangian corresponding to the Hamiltonian H , and the integral sign means

$$\int \rightarrow \int d^3x \int_0^\beta d\tau \quad (11.32)$$

for Euclidean time τ . Because the trace sums diagonal matrix elements, the boundary conditions on the Φ path integral are

$$\Phi(\vec{x}, \tau = 0) = \phi(\vec{x}) = \Phi(\vec{x}, \tau = \beta). \quad (11.33)$$

⁴ Except for strong effects coming from the coupling of a massive theory to the $K = 0$ sector, including effects from the Debye mass scale.

(For fermions, there is an extra minus sign.) So the quantum fields Φ are periodic (or antiperiodic, for fermions) in the time coordinate τ with period β . We can therefore write Φ as a Fourier sum,

$$\Phi(\vec{x}, \tau) = \sum_{-\infty}^{\infty} \phi_K(\vec{x}) e^{-i\omega_K \tau}, \tag{11.34}$$

with frequencies (called Matsubara frequencies) $\omega_K = 2\pi K T$. All Green's functions of Φ are similarly periodic. Inserting this periodic decomposition into \mathcal{L}_E exposes it as the sum over Euclidean field theories with K -dependent masses, as we said earlier. Moreover, the τ integral introduces a Kronecker delta function that conserves frequencies and an overall factor of β . When combined with the $1/g^2$ factor in \mathcal{L}_E , the $d = 3$ coupling becomes $g^2 T$.

The well-known Feynman rules for a thermal field theory differ in the treatment of the energy component of momentum, with the replacement

$$\begin{aligned} \frac{i}{2\pi} \int dk_0 &\rightarrow T \sum_K \\ 2\pi \delta\left(\sum k_0(j)\right) &\rightarrow \frac{1}{T} \delta_{0, \sum \omega_j}. \end{aligned} \tag{11.35}$$

The free-field thermal propagator for a massless scalar field is (aside from an irrelevant constant factor)

$$\Delta(\vec{x}, \tau) = \frac{T}{(2\pi)^3} \int d^3 p \sum_K e^{i\vec{p}\cdot\vec{x} - i\omega_K \tau} \frac{1}{-(i\omega_K)^2 + \omega_p^2}, \tag{11.36}$$

with $\omega_p = +\sqrt{|\vec{p}|^2 + m^2}$; this is a sum of Euclidean propagators with masses $\omega_K = 2\pi K T$. The sum over Matsubara frequencies yields

$$\Delta(\vec{x}, \tau) = \frac{1}{(2\pi)^3} \int \frac{d^3 p}{2\omega_p} e^{i\vec{p}\cdot\vec{x}} \{e^{-\omega_p \tau} [1 + n(\vec{p})] + e^{\omega_p \tau} n(\vec{p})\}, \tag{11.37}$$

where

$$n(\vec{p}) = \frac{1}{e^{\beta\omega_p} - 1} \tag{11.38}$$

is the Bose–Einstein occupation number. Similar formulas hold for fermions; we need not record them here.

11.7.1 The pinch technique in the zero-Matsubara-frequency sector

The first PT calculations for thermal field theory were done, as reported in Chapter 9, for $d = 3$ gauge theory or, in other words, the zero-Matsubara-frequency sector

[26, 27]. Note that when the Matsubara frequency is fixed, there is no question of the dependence of the result on τ , which can only be reliably estimated by a sum over all frequencies. In any case, the zero-frequency sector gives no τ dependence to the periodic thermal fields.

The computations were actually done in the light-cone gauge, which causes no problems because all dependence on the gauge-fixing vector n_μ cancels out before any integrations or sums are done. We translate the one-loop PT propagator of Eq. (9.1) to the thermal regime, with the result:

$$\widehat{d}(q, T) = \frac{1}{q^2 - \pi b_3 g^2 T q} \quad b_3 = \frac{15N}{32\pi}. \quad (11.39)$$

In later years, a number of people attempted to extract a running charge from their calculations, as we describe in the next section. The usual procedure is to choose a definition (which is not necessarily unambiguous) for a thermal running charge $g_T(q, T)$ and to define a beta function by

$$\beta_T = T \frac{dg_T(q, T)}{dT}. \quad (11.40)$$

From Eq. (11.39), we extract a zero-Matsubara-frequency running charge in one-loop perturbation theory as

$$g_T^2(q, T) = q^2 g^2 \widehat{d}(q, T) = \frac{g^2}{1 - 15g^2 T / (32q)}. \quad (11.41)$$

This yields

$$T \frac{dg_T(q, T)}{dT} = + \frac{15NTg_T^3}{64q}. \quad (11.42)$$

The derivative is positive because the running charge depends on T/q and the q derivative has the negative sign associated with infrared slavery. This means that the coupling constant runs away as T increases. Of course, this is equivalent to the infrared limit $q \rightarrow 0$, where we expect infrared-slavery diseases to arise.

This thermal β function, based as it is on one-loop perturbation theory in the zero-Matsubara-frequency sector, does not account for many important phenomena that are beyond the scope of this book. In particular, accounting for gluon electric masses in resummed internal propagators could, in principle, give rise to a term of $\mathcal{O}(g^4 T^2 / q^2)$, which is of higher order in the infrared limit $T \gg q$. Other corrections come from including a magnetic mass. These have been discussed by Elmfors and Kobes [22] using a general covariant background-field gauge; one important result of this work is that for any gauge parameter ξ , the $\mathcal{O}(g^4 T^2 / q^2)$ term vanishes. Although these authors did not realize that to find a gauge-invariant result, all we need to do is choose the Feynman background-field gauge $\xi = 1$, we do realize it.

When this is done and corrections from the magnetic mass are omitted, exactly the result of our Eq. (11.42) is found.

11.7.2 Developments in the full thermal field theory

Reference [28] gave the first PT calculation of the full thermal NAGT propagator at one-loop order. Again, the computations were done in the light-cone gauge. The result for the PT proper self-energy is (omitting the seagull graph that vanishes by dimensional integration)

$$\widehat{\Pi}_{\mu\nu} = \frac{1}{2}g^2NT \sum_K \int \frac{d^3k}{(2\pi)^3} \frac{1}{k^2(q+k)^2} \times [8(q^2\delta_{\mu\nu} - q_\mu q_\nu) + 2(2k+q)_\mu(2k+q)_\nu]. \tag{11.43}$$

The time component of the Euclidean four-vector k is $k_4 = 2\pi TK$. This self-energy is conserved and has two independent scalar pieces multiplying two tensorial structures; these are equivalent to calculating $\widehat{\Pi}_{44}$ and $\widehat{\Pi}_{ij}$. Most authors give results only for $q_4 = 0$, and we do the same; in the following results, q is a three-vector. After doing the integrals, one finds the renormalized propagator

$$(g^2\widehat{\Delta})_{44}^{-1} = bq^2 \ln\left(\frac{q^2}{\Lambda^2}\right) + \frac{NT^2}{\pi^2}P(\epsilon) \tag{11.44}$$

$$(g^2\widehat{\Delta})_{ij}^{-1} = \left(\delta_{ij} - \frac{q_i q_j}{q^2}\right) \left[bq^2 \ln\left(\frac{q^2}{\Lambda^2}\right) + \frac{NT^2}{\pi^2}Q(\epsilon) \right],$$

where

$$b = \frac{11N}{48\pi^2}; \quad \epsilon = \frac{q}{2T}, \tag{11.45}$$

and

$$P(\epsilon) = \frac{\pi^2}{3} + \frac{1}{2\epsilon} \int_0^\infty \frac{dy}{e^y - 1} \left[(y^2 - 4\epsilon^2) \ln \left| \frac{y + \epsilon}{y - \epsilon} \right| - 2y\epsilon \right] \tag{11.46}$$

$$Q(\epsilon) = \frac{1}{2} \int_0^\infty \frac{dy}{e^y - 1} \left[y - \frac{y^2 + 7\epsilon^2}{2\epsilon} \ln \left| \frac{y + \epsilon}{y - \epsilon} \right| \right].$$

In the infrared limit $q = 0$ (or $T = \infty$), we have $P(0) = \pi^2/3$ and $Q(0) = 0$. These correspond to the often-quoted perturbative values $m_e^2 = Ng^2T^2/3$ for the electric mass and zero for the magnetic mass m_m , respectively. However, the kinetic term $q^2 \ln(q^2/\Lambda^2)$ is not well behaved at small q at the one-loop level, and the interpretation of the electric mass requires resummations that replace $\ln q^2$ by something like $\ln(q^2 + 4m^2)$, which accounts for masses on the internal lines. We

will not discuss that interesting problem any further. In any event, as is well known, an electric mass arises at the one-loop level, but the magnetic mass vanishes to all orders in perturbation theory, despite that $m_m^2 \sim (Ng^2)^2 T^2$ looks like a fourth-order effect. Of course, the magnetic mass is nothing but the $d = 3$ dynamical gluon mass for which we argued in Chapter 9.

The next work that explicitly invoked the pinch technique to achieve gauge invariance in a thermal NAGT was an attempt to calculate the plasmon damping rate gauge invariantly [29]. Earlier gauge-dependent calculations gave a negative damping rate, which is a physical impossibility in any covariant gauge. Other calculations with other methods and in other gauges gave a positive damping coefficient. Finally, Nadkarni [29], using the results of Cornwall et al. [28], as stated in Eq. (11.43), found a one-loop PT damping rate that was unambiguously gauge invariant and also unambiguously negative. It was clear that this negative sign was precisely that arising from asymptotic freedom and that – as Nadkarni suggested – other, possibly nonperturbative effects needed to be included to get a positive rate. In an independent development, Braaten and Pisarski [23, 24, 25] developed an algorithm for resumming so-called hard thermal loops and using it to find a positive and gauge-invariant plasmon damping rate. An amplitude with external lines whose momenta p are soft (of order of the electric mass $\mathcal{O}(gT)$), coupled to a loop with hard loop momenta (of order $\mathcal{O}(T)$), has terms characterized by a dimensionless parameter $\mathcal{O}(g^2 T^2/p^2)$ that is of order unity and contributes at the same order as the soft tree-level amplitude. Here a factor $g^2 T$ comes from the coupling, and another power of T in the numerator comes from hard loop momenta. It is perhaps not surprising that the sum of all such hard loops is gauge invariant, as Braaten and Pisarski proved, because they are all of the same order in the coupling. With this process of resummation, these authors found a positive and gauge-invariant plasmon damping rate.

Braaten and Pisarski made no reference to the pinch technique, although their arguments would strongly suggest PT principles to those familiar with them. A few years later, Sasaki [30, 31, 32] made this connection. First, he calculated [30, 31] a thermal β function using the pinch technique, checking that he found the same result in four distinct gauge families, including the background-field gauges. Then he [32] showed that using the one-loop PT propagator with resummed internal propagator lines also coming from the PT actually yielded precisely Braaten and Pisarski's result for the plasmon damping rate.

We quote here Sasaki's result for the thermal β function, as defined through the running charge g_r of Eq. (11.41). He finds that

$$T \frac{dg_{TS}}{dT} = + \frac{14NTg^3}{64q}, \quad (11.47)$$

which is hardly different from what was found from the $d = 3$ PT propagator, as shown in Eq. (11.42), which has 15 rather than 14 in the numerator. This perhaps surprisingly small difference may arise because Sasaki used the full thermal PT propagator rather than just its zero-frequency part, as we did in Eq. (11.42). (But remember that this β function is infrared dominated, and so the zero-frequency sector should give the largest contribution.) The development of the plasmon damping rate would take us too far afield here, and we refer the reader to Sasaki's papers.

In thermal NAGTs, just as in NAGTs at zero temperature, the pinch technique does not solve difficult physics problems, but it does make it possible to separate true physics issues from gauge artifacts. No one should be surprised that mere use of the pinch technique itself at some low order of perturbation theory [29] does not give physical results in an asymptotically free theory; it is this unphysicality that ultimately drives the formation of a dynamical gluon mass and requires a self-consistent formulation of these gauge theories, such as we have argued for throughout this book. The demonstration that the resummation of hard thermal loops is equivalent to a PT resummation should not be a surprise either. The fact that Braaten and Pisarski did not recognize the connection of their earlier work to the pinch technique should not lull the reader into thinking that there is no connection to the pinch technique, as Sasaki showed.

11.8 Hints of supersymmetry in the pinch technique Green's functions

Let us now focus on a very interesting property of the one-loop PT three-gluon vertex discovered recently by Binger and Brodsky [33]. These authors first added quark and scalar loops to $\widehat{\Gamma}_{\alpha\mu\nu}^{amn}(q_1, q_2, q_3)$; this is straightforward from the point of view of gauge independence and gauge invariance because these loops are automatically gauge-fixing parameter independent and satisfy the Ward identity (Eq. (1.92)). All resulting one-loop integrals, including those of Eqs. (1.85) and (1.86), were evaluated for the first time, thus determining the precise tensorial decomposition of $\widehat{\Gamma}_{\alpha\mu\nu}^{amn}(q_1, q_2, q_3)$. Then, after choosing a convenient tensor basis, $\widehat{\Gamma}_{\alpha\mu\nu}^{amn}(q_1, q_2, q_3)$ was expressed as a linear combination of 14 independent tensors, each multiplied by its own scalar form factor. Every form factor receives, in general, contributions from gluons (G), quarks (Q), and scalars (S). It turns out that these three types of contributions satisfy very characteristic relations that are closely linked to supersymmetry and conformal symmetry and, in particular, the $\mathcal{N} = 4$ nonrenormalization theorems. For all form factors F (in d -dimensions), it was shown that

$$F_G + 4F_Q + (10 - d)F_S = 0, \quad (11.48)$$

which encodes the vanishing contribution of the $\mathcal{N} = 4$ supermultiplet in $d = 4$. Similar relations have been found in the context of supersymmetric scattering amplitudes [34, 35].

It should be emphasized that relations such as Eq. (11.48) do not exist for the gauge-dependent three-gluon vertex (see, e.g., Davydychev et al. [36]) because the gluon contributions depend on the gauge-fixing parameter, whereas the quarks and scalars do not. Indeed, it is uniquely the PT (or, equivalently, in the background Feynman gauge, $\xi_Q = 1$) Green's function that satisfies this homogeneous sum rule. Most important, calculating in the background field method with $\xi_Q \neq 1$ leads to a nonzero rhs of Eq. (11.48).

As was explained in detail by Binger and Brodsky, this type of relation hints at supersymmetry. To appreciate this point, it is useful to consider various supersymmetries in $d = 4$, as was done in [33]. Specifically, one may distinguish the following three cases, depending on the number \mathcal{N} of supersymmetries:

1. $\mathcal{N} = 1$: From the preceding definitions, it is clear that a vector superplet V_1 (gluons plus gluinos) contributes $ig^2 N_c (F_G + F_Q) \equiv ig^2 N_c F_{V_1}$ to a generic form factor F , whereas N_Φ chiral superplets contribute $ig^2 N_\Phi (\frac{1}{2} F_Q + F_S) \equiv ig^2 N_\Phi F_\Phi$. By the sum rule Eq. (11.48) in $d = 4$, we have $F_{V_1} + 6F_\Phi = 0$. Thus, any form factor can be written as

$$F = ig^2 (N_c F_{V_1} + N_\Phi F_\Phi) = \frac{ig^2}{3} \beta_0^{(N=1)} F_{V_1}, \tag{11.49}$$

where $\beta_0^{(N=1)} = 3N_c - 1/2N_\Phi$ is the first coefficient of the β function. Hence the contributions of vector and chiral superplets have precisely the same functional form for each form factor. Furthermore, every form factor is proportional to β_0 , even though all but one of them are ultraviolet finite.

2. $\mathcal{N} = 2$: In this case, the vector superplet gives $ig^2 N_c (F_G + 2F_Q + 2F_S) \equiv ig^2 N_c F_{V_2}$, whereas N_h hyperplets (a Weyl fermion of each helicity plus a doublet of complex scalars) yield $ig^2 N_h (F_Q + 2F_S) \equiv ig^2 N_h F_h$. The sum rule of Eq. (11.48) can be written as $F_{V_2} + 2F_h = 0$, and thus

$$F = ig^2 (N_c F_{V_2} + N_h F_h) = \frac{ig^2}{2} \beta_0^{(N=2)} F_{V_2}, \tag{11.50}$$

where $\beta_0^{(N=2)} = 2N_c - N_h$.

3. $\mathcal{N} = 4$: Now the vector superplet (the only multiplet allowed) contributes $2ig^2 N_c (F_G + 4F_Q + 6F_S) \equiv N_c F_{V_4}$, which is identically zero by the sum rule, which, of course, is a consequence of $\beta_0^{(N=4)} = 0$.

Thus, the similarities between form factors in $d = 4$ are related to supersymmetric nonrenormalization theorems. In particular, the exact conformal invariance of $\mathcal{N} = 4$ implies that the gauge-invariant, three-gluon Green's function is not renormalized at any order in perturbation theory. In fact, at one-loop order, there are not even finite corrections, as reflected in Eq. (11.48).

References

- [1] J. Papavassiliou and A. Pilaftsis, Effective charge of the Higgs boson, *Phys. Rev. Lett.* **80** (1998) 2785.
- [2] E. de Rafael, Lectures on quantum electrodynamics: 1, GIFT lectures given at Barcelona, Spain (1976).
- [3] J. Papavassiliou, E. de Rafael, and N. J. Watson, Electroweak effective charges and their relation to physical cross sections, *Nucl. Phys.* **B503** (1997) 79.
- [4] M. Bilenky, J. L. Kneur, F. M. Renard, and D. Schildknecht, Trilinear couplings among the electroweak vector bosons and their determination at LEP-200, *Nucl. Phys.* **B409** (1993) 22.
- [5] M. Binger and S. J. Brodsky, Physical renormalization schemes and grand unification, *Phys. Rev.* **D69** (2004) 095007.
- [6] K. Hagiwara, S. Matsumoto, D. Haidt, and C. S. Kim, A novel approach to confront electroweak data and theory, *Z. Phys.* **C64** (1994) 559.
- [7] J. S. Schwinger, On quantum electrodynamics and the magnetic moment of the electron, *Phys. Rev.* **73** (1948) 416.
- [8] E. N. Argyres, G. Katsilieris, A. B. Lahanas, C. G. Papadopoulos, and V. C. Spanos, One loop corrections to three vector boson vertices in the standard model, *Nucl. Phys.* **B391** (1993) 23.
- [9] J. Papavassiliou and K. Philippides, Gauge invariant three boson vertices in the standard model and the static properties of the W , *Phys. Rev.* **D48** (1993) 4255.
- [10] J. Papavassiliou, Gauge invariant proper self-energies and vertices in gauge theories with broken symmetry, *Phys. Rev.* **D41** (1990) 3179.
- [11] J. Bernabeu, L. G. Cabral-Rosetti, J. Papavassiliou, and J. Vidal, On the charge radius of the neutrino, *Phys. Rev.* **D62** (2000) 113012.
- [12] J. Bernabeu, J. Papavassiliou, and J. Vidal, On the observability of the neutrino charge radius, *Phys. Rev. Lett.* **89** (2002) 101802.
- [13] J. Bernabeu, J. Papavassiliou, and J. Vidal, The neutrino charge radius is a physical observable, *Nucl. Phys.* **B680** (2004) 450.
- [14] J. M. Cornwall, D. N. Levin, and G. Tiktopoulos, Derivation of gauge invariance from high-energy unitarity bounds on the S -matrix, *Phys. Rev.* **D10** (1974) 1145 [Erratum, *ibid.* **D11** (1975) 972].
- [15] J. Papavassiliou and A. Pilaftsis, Gauge invariance and unstable particles, *Phys. Rev. Lett.* **75** (1995) 3060.
- [16] J. Papavassiliou and A. Pilaftsis, A gauge independent approach to resonant transition amplitudes, *Phys. Rev.* **D53** (1996) 2128.
- [17] J. Papavassiliou and A. Pilaftsis, Gauge-invariant resummation formalism for two point correlation functions, *Phys. Rev.* **D54** (1996) 5315.
- [18] J. Papavassiliou, The pinch technique approach to the physics of unstable particles, paper presented at the 6th Hellenic School and Workshop on Elementary Particle Physics, Corfu, Greece (1998).

- [19] A. Denner, G. Weiglein, and S. Dittmaier, Application of the background field method to the electroweak standard model, *Nucl. Phys.* **B440** (1995) 95.
- [20] J. Papavassiliou, Asymptotic properties of Born-improved amplitudes with gauge bosons in the final state, *Phys. Rev.* **D60** (1999) 056001.
- [21] D. J. Gross, R. D. Pisarski, and L. G. Yaffe, QCD and instantons at finite temperature, *Rev. Mod. Phys.* **53** (1981) 43.
- [22] P. Elmfors and R. Kobes, The thermal beta function in Yang-Mills theory, *Phys. Rev.* **D51** (1995) 774.
- [23] E. Braaten and R. D. Pisarski, Resummation and gauge invariance of the gluon damping rate in hot QCD, *Phys. Rev. Lett.* **64** (1990) 1338.
- [24] E. Braaten and R. D. Pisarski, Soft amplitudes in hot gauge theories: A general analysis, *Nucl. Phys.* **B337** (1990) 569.
- [25] E. Braaten and R. D. Pisarski, Deducing hard thermal loops from Ward identities, *Nucl. Phys.* **B339** (1990) 310.
- [26] J. M. Cornwall, Nonperturbative mass gap in continuum QCD, paper presented at the French–American Seminar on Theoretical Aspects of Quantum Chromodynamics, Marseille, France (1981).
- [27] J. M. Cornwall, Dynamical mass generation in continuum QCD, *Phys. Rev.* **D26** (1982) 1453.
- [28] J. M. Cornwall, W. S. Hou, and J. E. King, Gauge-invariant calculations in finite-temperature QCD: Landau ghost and magnetic mass, *Phys. Lett.* **B153** (1985) 173.
- [29] S. Nadkarni, Linear response and plasmon decay in hot gluonic matter, *Phys. Rev. Lett.* **61** (1988) 396.
- [30] K. Sasaki, Gauge-independent thermal β function in Yang-Mills theory, *Phys. Lett.* **B369** (1996) 117.
- [31] K. Sasaki, Gauge-independent thermal β function in Yang-Mills theory via the pinch technique, *Nucl. Phys.* **B472** (1996) 271.
- [32] K. Sasaki, Gauge-independent resummed gluon self-energy in hot QCD, *Nucl. Phys.* **B490** (1997) 472.
- [33] M. Binger and S. J. Brodsky, The form factors of the gauge-invariant three-gluon vertex, *Phys. Rev.* **D74** (2006) 054016.
- [34] Z. Bern, L. J. Dixon, D. C. Dunbar, and D. A. Kosower, One-loop n -point gauge theory amplitudes, unitarity and collinear limits, *Nucl. Phys.* **B425** (1994) 217.
- [35] Z. Bern, L. J. Dixon, D. C. Dunbar, and D. A. Kosower, Fusing gauge theory tree amplitudes into loop amplitudes, *Nucl. Phys.* **B435** (1995) 59.
- [36] A. I. Davydychev, P. Osland, and O. V. Tarasov, Three-gluon vertex in arbitrary gauge and dimension, *Phys. Rev.* **D54** (1996) 4087 [Erratum, *ibid.* **D59** (1999) 109901].

